

COLOR ME INTRIGUED:
THE DISCOVERY OF iPTF 16fnn, A SUPERNOVA 2002CX-LIKE OBJECT

A. A. MILLER^{1,2,3*}, M. M. KASLIWAL³, Y. CAO⁴,
A. GOOBAR⁵, S. KNEŽEVIĆ⁶, R. R. LAHER⁷, R. LUNNAN³, F. J. MASCI⁷, P. E. NUGENT^{8,9}, D. A. PERLEY^{10,11},
T. PETRUSHEVSKA⁵, R. M. QUIMBY¹², U. D. REBBAPRAGADA¹³, J. SOLLERMAN¹⁴, F. TADDIA¹⁴, & S. R. KULKARNI³

DRAFT March 23, 2017

ABSTRACT

Modern wide-field, optical time-domain surveys must solve a basic optimization problem: maximize the number of transient discoveries or minimize the follow-up needed for the new discoveries. Here, we describe the *Color Me Intrigued* experiment, the first from the intermediate Palomar Transient Factory (iPTF) to search for transients simultaneously in the g_{PTF} - and R_{PTF} -bands. During the course of this experiment we discovered iPTF 16fnn, a new member of the 02cx-like subclass of type Ia supernovae (SNe). iPTF 16fnn peaked at $M_{g_{\text{PTF}}} = -15.09 \pm 0.17$ mag, making it the second least-luminous known type Ia SN. iPTF 16fnn exhibits all the hallmarks of the 02cx-like class: (i) low luminosity at peak, (ii) low ejecta velocities, and (iii) a non-nebular spectra several months after peak. Spectroscopically, iPTF 16fnn exhibits a striking resemblance to 2 other low-luminosity 02cx-like SNe: SNe 2007qd and 2010ae. iPTF 16fnn and SN 2005hk decline at nearly the same rate, despite a 3 mag difference in brightness at peak. When considering the full subclass of 02cx-like SNe, we do not find evidence for a tight correlation between peak luminosity and decline rate in either the g' or r' band. We further examine the $g' - r'$ evolution of 02cx-like SNe and find that their unique color evolution can be used to separate them from 91bg-like and normal type Ia SNe. This selection function will be especially important in the spectroscopically incomplete Zwicky Transient Facility/Large Synoptic Survey Telescope era. We measure the relative rate of 02cx-like SNe to normal SNe Ia and find $r_{N_{02cx}/N_{Ia}} = 25^{+75}_{-18.5}\%$. Finally, we close by recommending that LSST periodically evaluate, and possibly update, its observing cadence to maximize transient science.

Keywords: methods: observational – surveys – supernovae: general – supernovae: individual (SN 2002cx, SN 2005hk, iPTF 16fnn)

1. INTRODUCTION

The proliferation of large-area optical detectors has led to a recent renaissance of time-domain astronomy, and, in particular, the search for exotic transients. Over the

past ~decade, new surveys have dramatically increased the number of transients discovered on a nightly basis, and these efforts will culminate with the Large Synoptic Survey Telescope (LSST) in the early 2020s, which will discover 2,000 new supernovae (SNe) per night (Ivezić et al. 2008). Discovery is a small first step in improving our understanding of SNe. Detailed follow-up observations, either photometry spanning the ultraviolet, optical and infrared (UVOIR) or spectra, are needed to reveal the nature of these explosions (see Filippenko 1997 for a review of SNe spectra). Existing follow-up facilities are already taxed by the current rate of transient discovery, meaning the LSST-enabled two orders of magnitude increase in the discovery rate poses a serious “follow-up problem.” Namely, there will be substantially more known SNe than available resources to study them all in detail.

All transient surveys are forced to make a decision regarding the trade-off between discovery potential and the need for follow-up resources. For example, to maximize the number of transient discoveries, a survey should observe as wide an area as possible in a single filter. Implicit in this strategy is the need for outside follow-up resources. If, on the other hand, follow-up resources are scarce or prohibitively expensive, a survey may choose to repeatedly observe the same fields in different passbands to obtain color information. This would, however, reduce the total number of transient discoveries. Both strategies are employed by modern surveys. Broadly speaking,

¹ Center for Interdisciplinary Exploration and Research in Astrophysics (CIERA) and Department of Physics and Astronomy, Northwestern University, 2145 Sheridan Road, Evanston, IL 60208, USA

² The Adler Planetarium, Chicago, IL 60605, USA

³ Division of Physics, Mathematics, and Astronomy, California Institute of Technology, Pasadena, CA 91125, USA

⁴ eScience Institute and Astronomy Department, University of Washington, Seattle, WA 98195, USA

⁵ The Oskar Klein Centre, Department of Physics, AlbaNova, SE-106 91 Stockholm, Sweden

⁶ Department of Particle Physics and Astrophysics, Weizmann Institute of Science, Rehovot 7610001, Israel

⁷ Infrared Processing and Analysis Center, California Institute of Technology, Pasadena, CA 91125, USA

⁸ Lawrence Berkeley National Laboratory, Berkeley, California 94720, USA

⁹ University of California – Berkeley, Berkeley, CA 94720, USA

¹⁰ Dark Cosmology Centre, Niels Bohr Institute, University of Copenhagen, Juliane Maries Vej 30, DK-2100 København Ø, Denmark

¹¹ Liverpool John Moores University, Department of Astronomy, Liverpool, L3 5RF, UK

¹² Department of Astronomy, San Diego State University, San Diego, CA 92182, USA

¹³ Jet Propulsion Laboratory, California Institute of Technology, Pasadena, CA 91109, USA

¹⁴ The Oskar Klein Centre, Department of Astronomy, AlbaNova, SE-106 91 Stockholm, Sweden

* E-mail: amiller@northwestern.edu

shallow surveys tend to observe in a single filter [e.g., the All-Sky Automated Survey for Supernova (ASAS-SN; Shappee et al. 2014); the Palomar Transient Factory (PTF; Law et al. 2009)], while deeper surveys sacrifice area for color [e.g., the Supernova Legacy Survey (SNLS; Astier et al. 2006); the Panoramic Survey Telescope and Rapid Response System 1 (PS1) Medium Deep Survey (MDS; Chambers et al. 2016), the Dark Energy Survey Supernova search (DES SN survey; Kessler et al. 2015)]. The looming LSST “follow-up problem” has led to an increasing number of recent studies that consider only the photometric evolution of transients (e.g., Jones et al. 2016).

The intermediate Palomar Transient Factory (iPTF; Kulkarni 2013), which succeeded PTF,¹⁶ is a time-domain survey that has been conducted as a series of experiments. Like its predecessor, iPTF searched for transients using a single filter while obtaining two observations per field per night to reject asteroids from the transient candidate stream. Here, we describe the *Color Me Intrigued* experiment from the final semester of iPTF. This experiment was the first from PTF/iPTF to search for transients with multiple filters, though this color information was achieved with no loss of efficiency as the experiment still obtained two observations per field per night.

To our knowledge, *Color Me Intrigued* is the first transient experiment to employ both near-simultaneous color observations, g_{PTF} and R_{PTF} in this case, and a 1-d search cadence. Many high- z type Ia SN surveys have obtained near-simultaneous colors (often in as many as 5 filters), though the revisit time is always greater than 1 d, and typically ~ 3 –5 d (e.g., SNLS, Astier et al. 2006; the Sloan Digital Sky Survey-II Supernova Survey, Frieman et al. 2008; DES SN survey, Kessler et al. 2015). The ASAS-SN survey searches for transients with a 2-d cadence, but all ASAS-SN observations are obtained in a single broadband filter Shappee et al. 2014. The closest comparison to the *Color Me Intrigued* search strategy was that employed by the PS1 MDS. PS1 MDS obtained images of 10 separate ~ 7 deg² fields, every night a given field was visible. During dark time, observations would be obtained in both the g' and r' filters on the same night with a 3-d cadence (Chambers et al. 2016). On the first and second nights following $g'r'$ observations, PS1 MDS would observe exclusively in the i' and z' filters, respectively. Thus, while PS1 MDS had a 1-d cadence, near-simultaneous colors were obtained at best every 3 nights.

During the course of the *Color Me Intrigued* experiment, iPTF discovered a rare SN 2002cx-like object (hereafter 02cx-like SN), iPTF 16fmm. We discuss this SN in detail below.

1.1. Peculiar 02cx-like SNe

The discovery of an accelerating universe (Riess et al. 1998; Perlmutter et al. 1999) has led to numerous and extensive observational and theoretical studies into the nature of type Ia SNe over the past two decades. Despite

these efforts, a precise understanding of the nature and exact explosion mechanism for SN Ia progenitor systems is still unknown. While there is strong observational evidence that at least some SNe Ia come from white dwarf (WD) systems (e.g., Bloom et al. 2012a), and a general consensus that carbon/oxygen WDs give rise to type Ia SNe, there is ambiguity in the mechanisms and scenarios that lead to explosion (e.g., Hillebrandt et al. 2013). The multitude of observational campaigns designed to capture large samples of type Ia SNe for cosmological studies have also revealed several peculiar hydrogen-poor SNe (see Kasliwal 2012 and references therein). While these peculiar SNe retain many similarities to normal type Ia SNe, their distinct properties allow for the possibility of more extreme or unusual WD progenitor scenarios.

To date, the most common sub-class of peculiar SNe Ia are those similar to SN 2002cx (Li et al. 2003), of which there are now ~ 2 dozen known examples (e.g., Foley et al. 2013). The 02cx-like¹⁷ class is characterized by low ejecta velocities (\sim half normal SNe Ia) and low luminosities, ranging from $M \approx -19$ to -14 mag at peak. The distribution of host-galaxy morphologies for 02cx-like SNe is strongly skewed towards late-type hosts (e.g., Foley et al. 2013; White et al. 2015 and references therein), which may indicate massive star progenitors for this class (e.g., Valenti et al. 2009; Moriya et al. 2010). However, the maximum-light spectrum of SN 2008ha shows clear evidence for carbon/oxygen burning, providing a strong link between 02cx-like SNe and WD progenitors (Foley et al. 2010).

While the sample of 02cx-like SNe is relatively small, they constitute a significant fraction of the total number of type Ia SNe, ~ 5 –30% (Li et al. 2011; Foley et al. 2013; White et al. 2015). Multiple efforts have been made to identify simple correlations between basic observational properties for the class (e.g., McClelland et al. 2010; Foley et al. 2013), in part to aid the identification of a likely progenitor scenario. Significant outliers exist (e.g., Narayan et al. 2011), however, and the emerging consensus seems to be that 02cx-like SNe cannot be understood as a single parameter family (Magee et al. 2017).

Pure deflagration models are often invoked to explain the heterogeneity of the 02cx-like class (e.g., Phillips et al. 2007), as they can naturally explain the wide range in peak luminosity. As a result, extensive theoretical consideration has been given to these models recently (e.g., Kromer et al. 2013; Fink et al. 2014), with the express purpose of understanding 02cx-like SNe. Recently, Magee et al. (2016) compared early spectroscopic observations of SN 2015H, a member of the 02cx-class, to a deflagration model from Fink et al. (2014), and found good agreement. The model light curve evolves faster than the observations, though this may be reconciled with higher-ejecta-mass models (Magee et al. 2016). An interesting consequence of the pure deflagration models is that they do not completely unbind the WD, leaving a $\sim 1 M_{\odot}$ bound remnant (Kromer et al. 2013). Alternatively, Stritzinger et al. (2015) compared detailed observations of SN 2012Z, one of the most luminous members of the 02cx-like class, to pulsating delayed-detonation (PDD) models of exploding white dwarfs. In particu-

¹⁶ The initial PTF survey was conducted from 2009 Jul. through 2012 Dec. The iPTF survey was conducted from 2013 Feb. through 2016 Oct. Finally, the iPTF-extension was conducted from 2016 Nov. through 2017 Feb.

¹⁷ This subclass is sometimes alternatively referred to as type Iax SNe (Foley et al. 2013).

lar, [Stritzinger et al.](#) observe pot-bellied [Fe II] profiles in the near-infrared at late times, which are an indication of high-density burning. Based on this observation, and the direct comparison of model light curves and spectra, it is argued that SN 2012Z was a PDD explosion of a Chandrasekhar mass WD and not a pure deflagration ([Stritzinger et al. 2015](#)). While examining a large sample of low-velocity type I SNe, it is argued in [White et al. \(2015\)](#) that O2cx-like SNe are the result of double degenerate mergers, which may explain their observed heterogeneity as the masses of merging WDs can vary significantly. [White et al.](#) prefer pure deflagration models as an explanation for 2002es-like SNe, a low-velocity subclass of type Ia SNe that is distinct from the O2cx-like class ([Ganeshalingam et al. 2012](#); [Cao et al. 2016a](#)). Moving forward, it is clear that additional members of the O2cx-like class need to be found to disambiguate between pure deflagrations, PDD explosions, double degenerate mergers, and alternative scenarios.

Here, we present the discovery of a new member of the O2cx-like class, iPTF 16fNM. iPTF 16fNM was discovered in the course of the iPTF *Color Me Intrigued* experiment, and it was first identified as a possible low-velocity SN with spectra from the Spectral Energy Distribution Machine¹⁸ (SEDm; [Blagoradnova et al. 2017](#), in prep.). Our spectroscopic follow-up campaign clearly identifies iPTF 16fNM as an O2cx-like SN, which we show is one of the faintest known members of the class. The g_{PTF} and R_{PTF} light curves of iPTF 16fNM allow us to compare it, and several other O2cx-like SNe, to both normal and underluminous type Ia SNe.

2. COLOR ME INTRIGUED: THE IPTF TWO FILTER EXPERIMENT

The iPTF survey has been organized as a series of time-domain experiments conducted with the Palomar 48-in telescope (P48) selected on a semesterly basis. Proposals for individual experiments are written by members of iPTF institutions and selected by an internal time allocation committee. The decision to focus on a single experiment at a time was to minimize cadence interruptions and ensure a specific science goal could be accomplished. While the precise details (e.g., survey area, cadence, etc.) of the individual experiments varied, seasonal weather patterns and target availability constrained the possible science returns. As a result, experiments rotated on a roughly quarterly schedule with the following aims:¹⁹ (i) winter – persistent, but unpredictable, P48 weather closures led to wide-area surveys searching for intranight variability (e.g., [Cenko et al. 2013](#)) and/or rare, slowly evolving events (such as superluminous SNe), as it is otherwise difficult to maintain a night-to-night cadence, (ii) spring – smaller area surveys focused on maintaining a 1-d cadence to identify young SNe (e.g., [Cao et al. 2016b](#)), (iii) summer – wide-area surveys monitored the galactic plane (e.g., [Bellm et al. 2016](#)), and (iv) fall – 1-d cadence similar to the spring experiments.

Recognizing that the next generation Zwicky Transient Facility (ZTF; [Kulkarni 2016](#); [Bellm 2016](#)) would increase the discovery rate relative to PTF/iPTF by more than an

order of magnitude, we (AAM, YC, & MMK) proposed a ZTF pilot survey designed to reduce the “follow-up problem” for the final semester of iPTF. In brief, the proposed experiment, titled *Color Me Intrigued*, would be the first by PTF/iPTF to survey simultaneously in the g_{PTF} and R_{PTF} filters. Even with the advent of fast and efficient spectroscopic resources (e.g., SEDm), ZTF transient discoveries will outpace follow-up capabilities. Adopting a two filter strategy allows us to maximize the information content for each newly discovered transient, without compromising the overall survey area.

To reject asteroids as false positives in the search for transients, PTF/iPTF has always obtained a minimum of 2 observations of the same fields within a given night. These observations, typically separated by ~ 0.5 hr, could then reject moving objects by requiring transient candidates to have at least 2 co-spatial detections separated by $\gtrsim 0.5$ hr. Prior to *Color Me Intrigued*, these observations were always obtained in the same filter, with the initial PTF survey designed to observe in the g_{PTF} band during dark time and the R_{PTF} band during bright time ([Law et al. 2009](#)). *Color Me Intrigued* retained the basic 2 observations per field per night strategy, but instead observed once in g_{PTF} and once in R_{PTF} , regardless of moon phase. Thus, for the first time during PTF/iPTF all newly discovered transients would have quasi-simultaneous color coverage for the duration of their evolution. This color information reduces the “follow-up” problem in multiple ways. First, it enables an important triage of all newly discovered candidates, as the color provides an initial classification (e.g., [Poznanski et al. 2002](#)). Furthermore, the transients with the most extreme $g_{\text{PTF}} - R_{\text{PTF}}$ colors can immediately trigger follow-up observations. Second, for the subset of sources where follow-up observations prove impossible color curves greatly improve photometric classification. Finally, we note that few transients show intranight variability, meaning a second observation in the same filter only serves the purpose of rejecting moving objects. Changing filters accomplishes this same goal, while also adding information.

This two filter strategy needed to be tested via pilot survey prior to ZTF to address one major and one minor concern. The minor concern is that using two filters would somehow prevent the rejection of asteroids as non-transients. Given that asteroids are primarily rejected via their motion, however, filter choices should have no effect on our ability to identify genuine transients. Indeed, in practice we found that maintaining the requirement of two detections in the same night rejected asteroids from the transient-candidate stream. The major concern is that young transients may be missed due to (i) extreme colors, (ii) differences in the depth of the g_{PTF} and R_{PTF} observations, or (iii) a combination of the two. For example, most young transients are hot and therefore have blue $g_{\text{PTF}} - R_{\text{PTF}}$ colors. If the hot transient produces a faint detection in the g_{PTF} band, then there may be no corresponding detection in the R_{PTF} band, resulting in a non-detection. In this scenario the transient would have been detected with 2 g_{PTF} band observations. Additionally, iPTF g_{PTF} band observations reach a flux limit that is a factor of ~ 2 fainter than R_{PTF} band ([Law et al. 2009](#)). Thus, even relatively red sources ($g_{\text{PTF}} - R_{\text{PTF}} \gtrsim 0.5$ mag) detected near the g_{PTF} band

¹⁸ Documentation for SEDm is available here: <http://www.astro.caltech.edu/sedm/>.

¹⁹ Again, this is a broad overview which does not provide exact details of each experiment.

limit could be missed. A full systematic study of the biases introduced by the *Color Me Intrigued* strategy is beyond the scope of this paper, and will be addressed in a future study (A. A. Miller et al. 2017, in prep.). The discovery of 1-d old SNe and rare transients (e.g., iPTF 16fnl; Blagorodnova et al. 2017), however, suggests that the two-filter strategy does not significantly reduce the discovery potential of iPTF or ZTF.

The *Color Me Intrigued* experiment included 270 fields covering a total area of ~ 1940 deg². The experiment was conducted for 3 months, from 2017 Aug. 20 to Nov. 10, using the ~ 21 darkest nights during each lunation in that timeframe.²⁰ As a ZTF/LSST precursor the experiment adopted a rolling cadence strategy. The 270 fields were split into 3 groups of 90. During each lunation, one group would be observed with a 1-d cadence, while the other two would be observed with a 3-d cadence. Therefore each night 150 fields (90 from the 1-d cadence group and 60 from the 3-d cadence group) would be observed, yielding 300 total observations. Over the course of the experiment each field was slated to be observed 42 times, though weather losses ultimately reduced this number slightly. Adopting a rolling cadence strategy allowed us to obtain observations with a 1-d cadence, which is crucial for the study of young SNe, while maintaining a uniform survey depth over the 270 fields monitored.

In practice, scheduling constraints²¹ prevented us from observing the first set of 1-d cadence fields, those that were furthest west, during the third lunation of the experiment, 2017 Oct. 19 – Nov. 10. These fields were replaced by 90 new fields, which were observed with a 3-d cadence during the third lunation. This change in fields did not significantly affect the science output from the experiment, though it resulted in shorter duration P48 light curves for a subset of the newly discovered transients.

3. OBSERVATIONS OF iPTF 16fnm

3.1. Discovery

iPTF 16fnm, located at $\alpha_{J2000} = 01^{\text{h}}12^{\text{m}}38.32^{\text{s}}$, $\delta_{J2000} = +38^{\circ}30^{\text{m}}08.8^{\text{s}}$, was first detected by iPTF at $R_{\text{PTF}} = 20.23 \pm 0.17$ mag²² on 2016 Aug. 26.47 (UT dates are used throughout this paper). Following automated processing (Cao et al. 2016b; Masci et al. 2017) and the use of machine learning software that separates real transients from image subtraction artefacts, known as *realbogus* (Bloom et al. 2012b; Brink et al. 2013; Masci et al. 2017), the candidate was manually saved and internally designated iPTF 16fnm. The discovery image of iPTF 16fnm is shown in Figure 1.

The iPTF 16fnm host galaxy, UGC 00755, has a redshift $z_{\text{host}} = 0.02153$ (Wegner et al. 1993). Adopting

²⁰ The ~ 7 nights centered on full moon were used to complete the iPTF Census of the Local Universe H α survey (Cook et al. 2017).

²¹ Up to 20% of the available P48 observing time is reserved for the Caltech Optical Observatory every semester.

²² Photometry for iPTF 16fnm is reported in the g_{PTF} and R_{PTF} filters throughout, which are similar to the SDSS g' and r' filters, respectively (see Ofek et al. 2012 for details on PTF calibration). The correction from the g_{PTF} and R_{PTF} filters to SDSS g' and r' requires knowledge of the intrinsic source color (see Eqns. 1 and 2 in Ofek et al. 2012). 02cx-like SNe do not follow a standard spectral evolution, so the color terms for iPTF 16fnm are unknown.

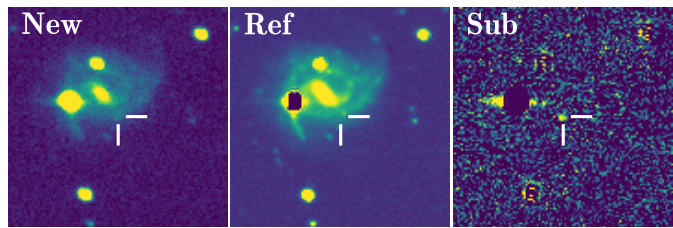


Figure 1. R -band discovery image of iPTF 16fnm showing the new, reference, and subtraction image from left to right. Images are shown on a linear scale with the saturation levels selected to highlight faint structure in the host galaxy, UGC 00755. North is up and east to the left, and the images are centered on the SN position as indicated by the crosshairs, which are $10''$ long.

$H_0 = 73$ km s⁻¹ Mpc⁻¹, and correcting for Virgo infall, this redshift corresponds to a distance $d = 90.5 \pm 6.3$ Mpc and distance modulus $\mu = 34.78 \pm 0.15$ mag (Mould et al. 2000). Thus, at the time of discovery iPTF 16fnm had an absolute magnitude $M_{R_{\text{PTF}}} \approx -14.5$ mag. The light curve peaked ~ 3 days later at $M \approx -15$ mag in both the g_{PTF} and R_{PTF} filters, suggesting iPTF 16fnm may be a “gap” transient (see Kasliwal 2011, 2012 and references therein).

The first spectrum of iPTF 16fnm was obtained on 2016 Sep. 03.25 with the SEDm integral field unit (IFU) spectrograph (Ben-Ami et al. 2012, Blagorodnova et al. 2017, in prep.) on the Palomar 60-inch telescope (P60). This spectrum showed low-velocity Si II absorption, which in conjunction with the relatively faint absolute magnitude suggested that iPTF 16fnm may be a sub-luminous 02cx-like SN, similar to SN 2008ha (Foley et al. 2009). Subsequent spectra obtained with larger aperture telescopes confirmed this initial classification.

3.2. Photometry

Photometric observations of iPTF 16fnm were conducted in the g_{PTF} and R_{PTF} bands using the PTF camera (Law et al. 2009) on the Palomar 48-inch telescope. The brightness of iPTF 16fnm was measured following image subtraction via point-spread-function (PSF) photometry with the PTFIDE software package (Masci et al. 2017). These measurements are summarized in Table 1, and shown in Figure 2. We only consider the SN detected in epochs where the signal-to-noise ratio (SNR) is ≥ 3 , while we otherwise conservatively report 5σ upper limits.

We determine the time of and brightness at maximum for iPTF 16fnm via second-order polynomial fits to the epochs when iPTF 16fnm was detected. From these fits we find that iPTF 16fnm peaked on HJD $2,457,629.8 \pm 2.0$ and $2,457,632.8 \pm 4.8$ at 19.87 ± 0.07 mag and 19.88 ± 0.05 mag, in the g_{PTF} - and R_{PTF} -bands, respectively. These measurements represent the observed maxima of iPTF 16fnm, and have not been corrected for Milky Way or host galaxy extinction. 02cx-like SNe do not follow a standard color evolution, meaning host-galaxy extinction cannot be inferred from photometry alone. We do not detect narrow Na I D at the redshift of UGC 00755 in any of our spectra, and therefore we assume that host-galaxy extinction is negligible. This assumption is supported by the observed blue color of iPTF 16fnm at peak.

Adopting the distance modulus to UGC 00755, and correcting for foreground Galactic extinction ($A_g = 0.178$ mag, $A_r = 0.123$ mag; Schlafly & Finkbeiner

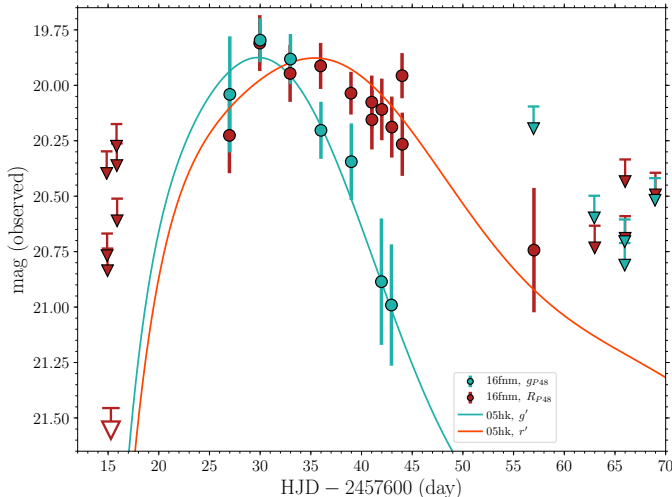


Figure 2. P48 light curves showing the evolution of iPTF 16fnm. Teal and crimson circles show detections in the g_{PTF} and R_{PTF} bands, respectively. 5σ upper limits are shown with downward arrows. The open downward arrow shows the 5σ upper limit from combining the 6 epochs taken ~ 11 -12 d prior to discovery. The solid teal and red-orange lines show polynomial fits to the g' and r' filter observations of SN 2005hk (Phillips et al. 2007). The curves have been shifted to align the time and brightness of maximum in g band for both SNe and stretched to match the redshift of iPTF 16fnm. The general agreement between the two suggests the rise time for iPTF 16fnm is similar to SN 2005hk, ~ 15 d.

2011), we find that iPTF 16fnm peaked at $M_{g_{\text{PTF}}} = -15.09 \pm 0.17$ mag and $M_{R_{\text{PTF}}} = -15.02 \pm 0.16$ mag, under the assumption of no local host extinction.

We cannot place strong observational constraints on the rise time of iPTF 16fnm: prior to its initial detection, iPTF had not observed this field for ~ 12 d (see Figure 2). If we combine the forced-PSF flux measurements from the 6 epochs taken between HJD 2,457,614 and 2,457,616, we derive a more constraining inverse-variance-weighted upper limit of $R_{\text{PTF}} > 21.46$ mag on HJD 2,457,615.3. This deeper non-detection suggests the rest-frame rise time of iPTF 16fnm is < 17.2 d in the R -band. Further constraints on the rise-time are available by comparing iPTF 16fnm and SN 2005hk, the O2cx-like SN with the best observational constraints on the time of explosion (Phillips et al. 2007). Figure 2 shows polynomial fits to the g' - and r' -band light curves of SN 2005hk, shifted to match the time and brightness of iPTF 16fnm in the g_{PTF} band and stretched to match the redshift of iPTF 16fnm. Formally, no further stretch factor is required to provide an excellent match between SN 2005hk and iPTF 16fnm, as can be seen in Figure 2. Assuming that SN 2005hk and iPTF 16fnm have similar compositions, opacities, and temperatures, which is reasonable based on the spectral similarities of the two supernovae, then the rise time of iPTF 16fnm is ~ 15 d (Phillips et al. 2007), consistent with our R_{PTF} observational constraints above.

Furthermore, a gap in our observations between ~ 13 and 27 d after g -band maximum make it difficult to properly measure the decline rate of iPTF 16fnm. If we adopt the same quadratic fit used to determine the time of g -band maximum to estimate the SN brightness beyond $+13$ d after maximum, then iPTF 16fnm declined by 1.75 ± 0.46 mag in the g_{PTF} band after 15 d in its rest frame. Using the same similarity ar-

Table 1
iPTF 16fnm P48 photometry

HJD - 2,457,600	mag ^a	σ_{mag}
<i>g</i> _{PTF}		
27.008	20.04	0.26
30.002	19.80	0.10
32.990	19.88	0.11
35.998	20.20	0.13
38.992	20.34	0.17
41.964	20.89	0.29
42.951	20.99	0.27
56.972	>20.10	...
62.963	>20.50	...
65.962	>20.71	...
65.963	>20.60	...
68.951	>20.42	...
<i>R</i> _{PTF}		
14.863	>20.30	...
14.905	>20.67	...
14.948	>20.74	...
15.833	>20.17	...
15.863	>20.26	...
15.892	>20.51	...
26.971	20.23	0.17
29.964	19.81	0.13
32.954	19.95	0.13
35.964	19.91	0.10
38.960	20.04	0.10
41.009	20.08	0.12
41.022	20.16	0.13
42.002	20.11	0.14
42.986	20.19	0.14
43.998	19.96	0.10
44.019	20.27	0.14
57.008	20.74	0.28
63.001	>20.63	...
66.001	>20.59	...
66.002	>20.33	...
68.991	>20.39	...

^a Observed mag, not corrected for Galactic extinction. 5σ upper limits are reported for epochs where iPTF 16fnm is not detected.

guments about SN 2005hk from above, then we would expect the two SNe to feature similar declines, meaning for iPTF 16fnm $\Delta m_{15}(B) \approx 1.6$ mag, as was found for SN 2005hk (Phillips et al. 2007).

3.3. Spectroscopy

Optical spectra of iPTF 16fnm were obtained on 2016 September 03.3 and 2016 September 07.3 with the SEDm on the Palomar 60-in telescope (P60). Additional spectra were obtained on 2016 September 03.4 with the double beam spectrograph (DBSP; Oke et al. 1995) on the Palomar 200-in telescope (P200), on 2016 September 06.1 and September 10.1 with the Andalucia Faint Object Spectrograph and Camera (ALFOSC) on the Nordic Optical Telescope (NOT), and on 2016 September 30.5 and November 28.4 with the low-resolution imaging spectrometer (LRIS; Oke & Gunn 1982) on the Keck I 10 m telescope. All spectra were extracted and calibrated using standard procedures. The sequence of iPTF 16fnm spectra is shown in Figure 3. A log of our spectroscopic observations is presented in Table 2.²³

iPTF 16fnm shows the hallmark features of O2cx-like SNe: low velocity lines of intermediate-mass and Fe-

²³ Our iPTF 16fnm spectra will be publically released via WIS-erep (Yaron & Gal-Yam 2012) following paper acceptance.

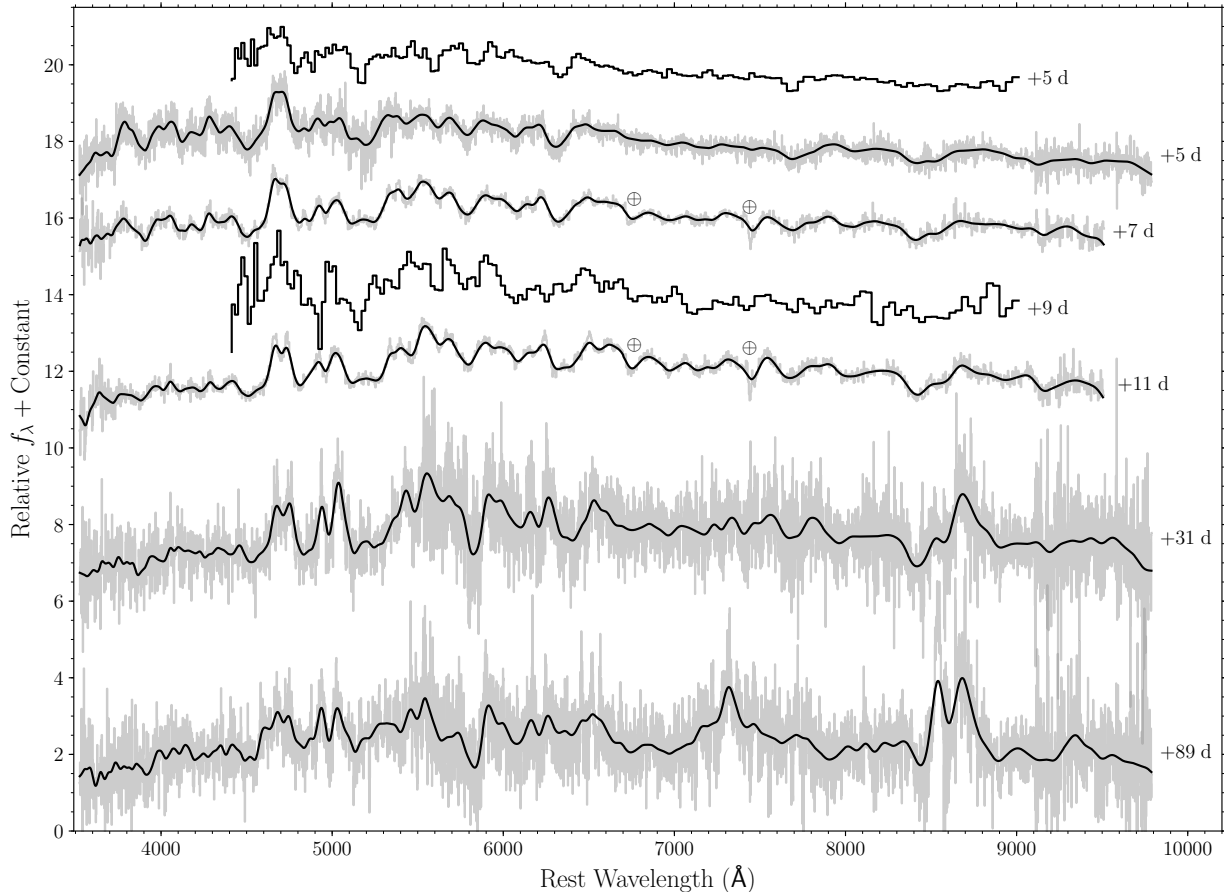


Figure 3. Spectral evolution of iPTF 16fm. The spectra are labeled with their ages in the rest frame of the SN relative to the observed g_{PTF} -band maximum on 2016 August 29.3. The raw spectra are shown in grey, while the solid black lines are convolved with a Gaussian filter with $\text{FWHM} = 2,500 \text{ km s}^{-1}$. The low SNR portion of SEDm spectra (+5 and +9) is trimmed blueward of 4500 \AA in the observer frame, and these spectra are not smoothed. From the first spectrum, iPTF 16fm exhibited low-velocity features characteristic of O2cx-like SNe.

Table 2
Log of Spectroscopic Observations

t^a (d)	UT Date	Instrument ^b	Range (\AA)	Exp ^c (s)	Air Mass
4.9	2016-09-03.25	SEDm	3806–9187	2700	1.51
5.0	2016-09-03.36	DBSP	3101–10236	1200	1.07
7.7	2016-09-06.13	ALFOSC	3427–9714	4800	1.02
8.8	2016-09-07.25	SEDm	3807–9187	2700	1.46
11.5	2016-09-10.06	ALFOSC	3556–9712	4800	1.10
31.5	2016-09-30.53	LRIS	3071–10297	975	1.14
89.1	2016-11-28.37	LRIS	3057–10276	3370	1.14

^a Age in rest-frame days relative to the observed g_{PTF} -maximum on 2016-08-29.298.

^b SEDm: Spectral Energy Distribution Machine on the Palomar 60-in telescope. DBSP: Double Beam Spectrograph on the 200-in Palomar Hale Telescope. ALFOSC: Andalusia Faint Object Spectrograph and Camera on the 2.6-m Nordic Optical Telescope. LRIS: low-resolution imaging spectrograph on the 10-m Keck-I telescope.

^c Exposure time.

group elements. In our earliest spectroscopic observations, taken within a week of g_{PTF} -band maximum, Si II $\lambda 6335$ shows an expansion velocity of only $\sim 2,000 \text{ km s}^{-1}$. Other relatively unblended lines, such as Ca H&K, Fe II $\lambda 4555$ and O I $\lambda 7774$ show expansion speeds

of $\sim 3,200 \text{ km s}^{-1}$.

The late time spectra of iPTF 16fm resemble the evolution of SN 2008ha. While the [Ca II] $\lambda\lambda 7291, 7323$ and Ca II NIR triplet are not as strong in iPTF 16fm as in SN 2008ha, they are clearly present, unlike in SN 2002cx. Furthermore, like SN 2008ha, absorption from Fe II $\lambda 4555$ is prominent more than a month after maximum. Finally, both iPTF 16fm and SN 2008ha exhibit a strong P Cygni profile at $\sim 5800 \text{ \AA}$, possibly associated Na D, for months after maximum light, even as the rest of the optical spectrum transitions to a nebular state.

We measure the expansion velocities for different species in iPTF 16fm by tracking the wavelength of the minimum for each feature, as shown in Figure 4. The measurements are made following a convolution of the spectra with a gaussian kernel with full-width half-max ($\text{FWHM}) = 2,000 \text{ km s}^{-1}$. Blending and the relatively low SNR of the spectra make it challenging to track the evolution of individual lines more than 10 days after g_{PTF} -band maximum. The Fe II $\lambda 4555$ feature shows a modest decrease of only $\sim 700 \text{ km s}^{-1}$ from +5 to +31 d. At +5 d after maximum the Na D feature exhibits significantly faster speeds of $\sim 5,200 \text{ km s}^{-1}$, decreasing to $\sim 2,800 \text{ km s}^{-1}$ at +89 d. The higher velocities for

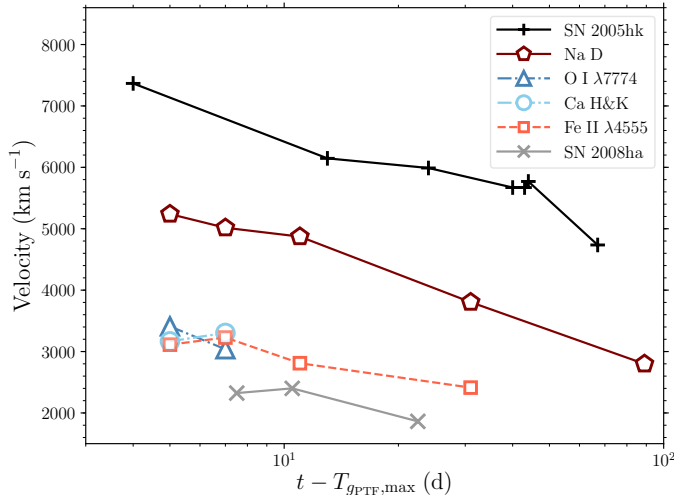


Figure 4. Velocity evolution of the absorption minimum of Ca H&K (circles), Fe II $\lambda 4445$ (squares), Na D (pentagons), O I $\lambda 7774$ (triangles) for iPTF 16fnn traced by the minimum of absorption. Also shown is the velocity evolution of SN 2005hk (pluses, as traced by Fe II $\lambda 4445$) and SN 2008ha (X symbols, as traced by O I $\lambda 7774$). The spectra for SN 2005hk and SN 2008ha are taken from Phillips et al. (2007) and Foley et al. (2009), respectively. iPTF 16fnn is clearly intermediate between SN 2005hk and SN 2008ha. For iPTF 16fnn the Na D doublet may be contaminated by other features affecting our velocity measurements.

this line indicates that our measurement may be contaminated by other features. Taken together, these lines demonstrate that iPTF 16fnn has a velocity structure that is intermediate between SN 2005hk, with typical velocities of $\sim 7,000 \text{ km s}^{-1}$ (Phillips et al. 2007), and SN 2008ha, with typical velocities of $\sim 2,000 \text{ km s}^{-1}$ (Foley et al. 2009; Valenti et al. 2009).

4. COMPARISON TO OTHER SUB-LUMINOUS O2CX-LIKE SNE

We compare the photometric evolution of iPTF 16fnn to other sub-luminous O2cx-like SNe in Figure 5. The comparison SNe are: SN 2007qd (McClelland et al. 2010), SN 2010ae (Stritzinger et al. 2014), and SN 2008ha (Stritzinger et al. 2014), all low luminosity O2cx-like SNe with g' - and r' -band photometric coverage.²⁴ Each light curve in Figure 5 has been corrected for foreground Galactic extinction using the Schlafly & Finkbeiner (2011) updates to the Schlegel et al. (1998) reddening maps. SN 2010ae has been further corrected for a host galaxy reddening of $E(B-V)_{\text{host}} = 0.50 \text{ mag}$ (Stritzinger et al. 2014; Foley et al. 2013). The light curves have been shifted to align the time of g' -band maximum, where we have assumed the first detection of SN 2007qd corresponds to g' -band maximum (see McClelland et al. 2010 for further details). We adopt distance moduli of 36.23, 30.44, and 31.64 mag for SN 2007qd, SN 2010ae, and SN 2008ha, respectively, which are corrected for Virgo infall (Mould et al. 2000) and assume $H_0 = 73 \text{ km s}^{-1} \text{ Mpc}^{-1}$. No K - or S -corrections have been applied.

Figure 5 shows that iPTF 16fnn is generally similar to SN 2010ae and SN 2007qd. In particular, all 3 SNe

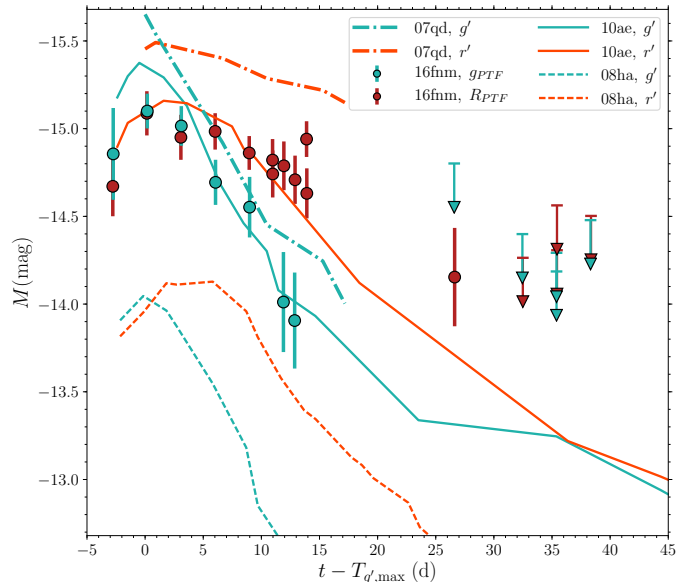


Figure 5. Photometric evolution of the faintest members of the O2cx-like class in the g' and r' filters. From brightest to faintest they are: SN 2007qd, SN 2010ae, iPTF 16fnn, and SN 2008ha. These SNe all feature fast declines in the g' band, $\Delta m_{15}(g) \gtrsim 1.2 \text{ mag}$. SN 2007qd and iPTF 16fnn, on the other hand, exhibit relatively slow declines in the r' filter.

are of comparable brightness at peak ($15 \text{ mag} \lesssim M \lesssim 15.5 \text{ mag}$), and exhibit a fast decline in the g' band. SN 2008ha, on the other hand, is significantly fainter than the other SNe. Interestingly, both iPTF 16fnn and SN 2007qd exhibit a slow decline in the R_{PTF}/r' band, evolving from $g' - r' \approx 0.1 \text{ mag}$ near peak to $g' - r' \approx 0.9 \text{ mag}$ at $t \approx 15 \text{ d}$.

We compare the same 4 SNe, as well as SN 2005hk, at similar epochs, $t \approx +4$ to $+10 \text{ d}$, in Figure 6. The spectra are ordered top to bottom from the most luminous to least luminous, though note that changes in host-galaxy reddening could re-arrange the middle 3 spectra. From Figure 6 it is clear that SN 2005hk has the highest velocity features, while SN 2007qd, SN 2010ae, and iPTF 16fnn all have similar velocities, and SN 2008ha has the lowest velocity signatures.²⁵ The overall similarity of SN 2007qd, SN 2010ae, and iPTF 16fnn is striking. These 3 SNe are clearly closely related with similar velocities and ejecta composition, which is dominated by intermediate mass elements. While the O2cx-class as a whole exhibits great diversity, SN 2007qd, SN 2010ae, and iPTF 16fnn feature nearly identical spectra and photometric evolution suggesting they had similar progenitors or explosion mechanisms.

5. RESULTS

While O2cx-like SNe exhibit a large range in luminosity (roughly 2 orders of magnitude separate SN 2008ha and SN 2009kr), their general similarity to normal Type Ia SNe have led many to search for correlated observational properties to unify the class. While the precise details of the explosion mechanism are debated, the observational consensus points to white dwarf (WD) progenitors for

²⁴ We remind the reader that iPTF 16fnn was observed in the g_{PTF} and R_{PTF} filters, which are similar to SDSS g' and r' (see Ofek et al. 2012 for the filter transformations).

²⁵ While these 5 SNe show an apparent correlation between absolute magnitude and velocity for O2cx-like SNe, SN 2009ku, the only O2cx-like SN with velocities as low as SN 2008ha, is also the most luminous O2cx-like SN (Narayan et al. 2011).

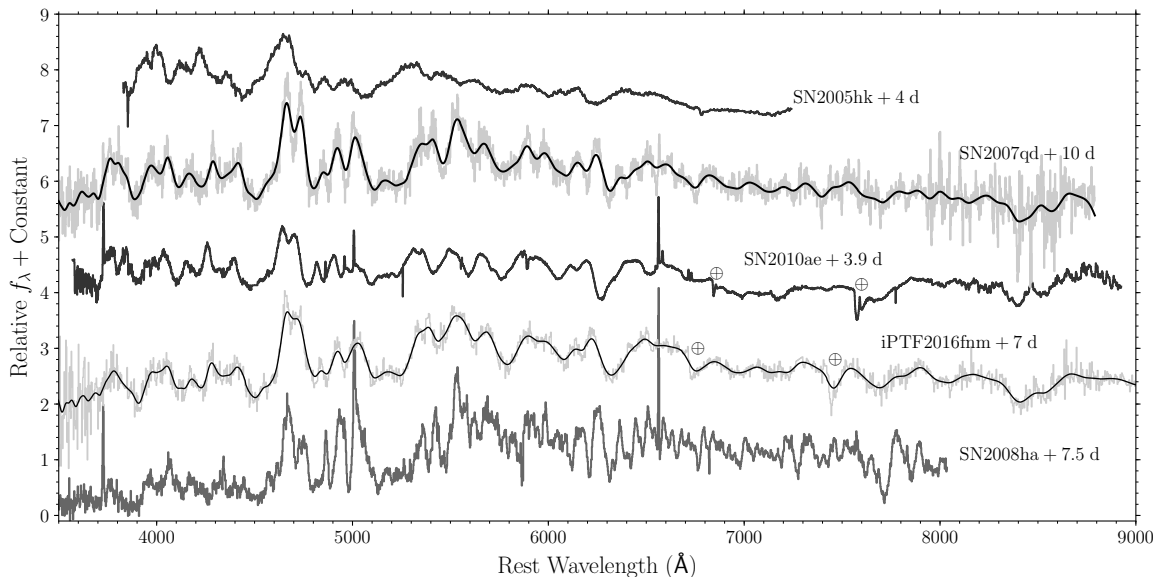


Figure 6. Spectral comparisons of iPTF 16fm to other subluminous O2cx-like SNe. The spectra are labeled with their ages in the rest frame of the SN relative to B - or g' -band maximum. SN 2007qd and iPTF 16fm are also shown following convolution with a FWHM = 2,500 km s⁻¹ gaussian kernel. From top to bottom, the spectra are SN 2005hk (Phillips et al. 2007), SN 2007qd (McClelland et al. 2010), SN 2010ae (Stritzinger et al. 2014), iPTF 16fm, and SN 2008ha (Foley et al. 2009). SN 2005hk is a prototypical O2cx-like SN, while SNe 2007qd and 2010ae, like iPTF 16fm, were fainter at the time of maximum brightness with lower expansion velocities. SN 2008ha is the faintest member of the O2cx-like class.

O2cx-like SNe (see e.g., Foley et al. 2013; Stritzinger et al. 2015; Magee et al. 2017). Thus, it may be the case that O2cx-like SNe are a single parameter family, much like type Ia SNe, whose evolution is largely controlled by the amount of ⁵⁶Ni synthesized during explosion (Mazzali et al. 2007).

Using the first four known O2cx-like SNe, SN 2002cx, SN 2005hk, SN 2007qd, and SN 2008ha, a potential correlation between absolute magnitude and ejecta velocity for O2cx-like SNe, whereby more luminous events also have faster ejecta, was identified in McClelland et al. (2010). The subsequent discovery of SN 2009ku (Narayan et al. 2011), which had extremely low velocities, like SN 2008ha, while also being the most luminous member of the class, poses a significant challenge to this correlation. While an increased sample of O2cx-like SNe shows a general correlation between ejecta velocity and luminosity (see Figure 20 in Foley et al. 2013), SN 2009ku remains a significant outlier.

5.1. The Luminosity–Decline Relation for O2cx-like SNe

Many studies have examined whether O2cx-like SNe follow their own Phillips relation, similar to type Ia SNe, whereby more luminous SNe Ia also have broader light curve shapes (Phillips 1993). Using a sample of 13 O2cx-like SNe, evidence for an anti-correlation between M_V and $\Delta m_{15}(V)$ is presented in Foley et al. (2013). The V -band $M - \Delta m_{15}$ relation presented in Foley et al. (2013) exhibited significant scatter, well in excess of that found for normal type Ia SNe. Furthermore, the sample in Foley et al. (2013) excludes SN 2007qd, which declined at a similar rate as SN 2005hk, despite being ~ 2.5 mag fainter at peak.²⁶

²⁶ SN 2007qd was first detected after g' -band maximum, which is why it was excluded from the sample in Foley et al. (2013). However, the 50 d range for the time of maximum for SN 2007qd in Table 5 of Foley et al. (2013) ignores the deep upper limits

iPTF 16fm provides additional evidence for the lack of a simple $M - \Delta m_{15}$ relation for O2cx-like SNe. In particular, Figure 2 shows that iPTF 16fm declined at a nearly identical rate as SN 2005hk, which peaked at $M_{g'} = -18.08 \pm 0.25$ mag (Stritzinger et al. 2015), 3 mag brighter than iPTF 16fm, $M_{g_{PTF}} = -15.08 \pm 0.17$ mag. To further illustrate this point, we update Figure 10 from White et al. (2015) to include iPTF 16fm, as shown in Figure 7. For O2cx-like SNe with available g' observations, we additionally include estimates of $M_{g'}$ and $\Delta m_{15}(g')$ using the same procedure adopted in White et al. (2015). Even if SN 2007qd is excluded from the sample, iPTF 16fm stands out as a strong outlier for any $M - \Delta m_{15}$ relation in the r'/R_{PTF} -band. Examining those sources with g' observations, Figure 7 shows weak evidence for a $M - \Delta m_{15}$ relation, though the scatter is extremely large. As already noted, SN 2005hk and iPTF 16fm exhibit similar decline rates but differ by ~ 3 mag at peak. Furthermore, SN 2005hk and SN 2009ku both peak at $M_{g'} \approx -18$ mag, yet their $\Delta m_{15}(g')$ differ by ~ 1 mag.

While a larger sample with better photometric coverage is still required, we conclude that the O2cx-like class of SNe cannot be well described by a single $M - \Delta m_{15}$ relation. As future time-domain surveys significantly increase the sample of known O2cx-like SNe, it may be the case that further subdivision of the O2cx-like class yields a subset that can be described by a simple $M - \Delta m_{15}$ relation.

5.2. A Selection Function for O2cx-like SNe: $g' - r'$ Color Evolution

reported in McClelland et al. (2010) between ~ 10 –20 d prior to SN 2007qd’s first detection. As argued in McClelland et al. (2010), the initial detection of SN 2007qd is very likely near the epoch of g' maximum.

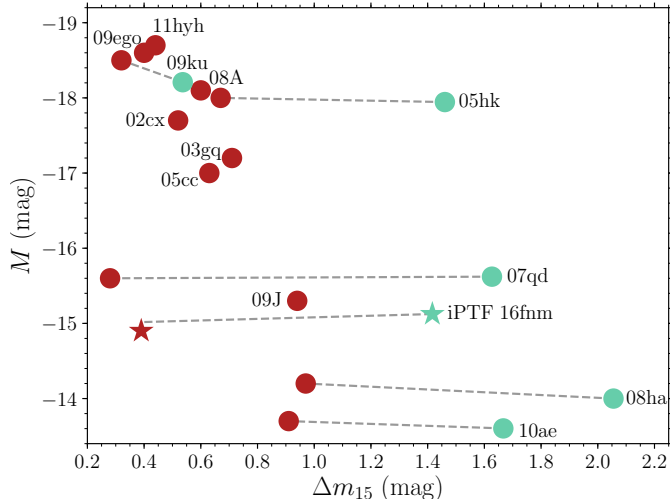


Figure 7. Absolute magnitude vs. Δm_{15} , both in the r' (shown in crimson) and g' -bands (teal) for O2cx-like SNe, adapted from White et al. (2015). The dashed grey lines connect SNe for which both r' and g' observations are available. Note that following White et al. (2015), we have not corrected M for host galaxy extinction, which is why SN 2010ae is fainter than SN 2008ha in this figure. In the r' band most O2cx-like SNe lie along a high-scatter sequence, though SN 2007qd and iPTF 16fnn are clear outliers. Similarly, g' -band observations of O2cx-like SNe also show weak evidence for a simple $M - \Delta m_{15}$ relation.

In Foley et al. (2013), the color evolution of O2cx-like SNe is examined to see if all O2cx-like SNe can be described by a single color curve following a reddening correction, similar to the Lira-law for normal type Ia SNe (Lira 1996; Phillips et al. 1999). Foley et al. apply reddening corrections to a sample of six O2cx-like SNe, and find a significant reduction in scatter for the $V - R$ and $V - I$ color curves. The same corrections do not reduce the $B - V$ scatter, however. As a result, they cannot conclude whether the observed scatter is the result of dust reddening or intrinsic differences in the class.

Here, we instead examine the color curves of O2cx-like SNe as a possible selection function to separate them from normal type Ia SNe. While O2cx-like SNe do not follow a $M - \Delta m_{15}$ relation, we find that the $g' - r'$ color evolution is relatively uniform for the class. In Figure 8, we show the $g' - r'$ color evolution for nine O2cx-like SNe, including: SN 2008ha (Stritzinger et al. 2014), SN 2010ae (Stritzinger et al. 2014), SN 2007qd (McClelland et al. 2010), SN 2005hk (Phillips et al. 2007), SN 2009ku (Narayan et al. 2011), PS1-12bwh (Magee et al. 2017), SN 2015H (Magee et al. 2016), SN 2012Z (Stritzinger et al. 2015), and iPTF 16fnn (where we are using g_{PTF} and R_{PTF} from this study as a proxy for g' and r' , respectively). Figure 8 also shows the color evolution of 35 normal type Ia SNe and 9 underluminous, 91bg-like type Ia SNe from Folatelli et al. (2013). Normal type Ia SNe are defined as those spectroscopically classified as normal by both the Supernova Identification package (SNID; Blondin & Tonry 2007) and via the method developed in Wang et al. (2009). 91bg-like SNe are defined as those classified as 91bg-like by SNID.

The light curves in Figure 8 have been normalized to the time of B -band maximum. For 3 (2) O2cx-like SNe: SN 2007qd, PS1-12bwh, and iPTF 16fnn (SN 2009ku, SN 2015H) the time of g' -band (r' -band) maximum is used as a proxy because B -band observations are not

available. Galactic reddening corrections have been applied to all light curves in Figure 8 using the Schlafly & Finkbeiner (2011) updates to the Schlegel et al. (1998) dust maps. The following host-galaxy reddening corrections have also been applied $E(B - V) = 0.09$ mag (Phillips et al. 2007), 0.50 mag (Stritzinger et al. 2014), 0.20 mag (Magee et al. 2017), and 0.07 mag (Stritzinger et al. 2015) for SN 2005hk, SN 2010ae, PS1-12bwh, and SN 2012Z, respectively. The remaining 5 O2cx-like SNe do not show evidence of Na I D absorption at the redshift of the host galaxy (Foley et al. 2009; McClelland et al. 2010; Narayan et al. 2011; Magee et al. 2016), and we therefore make no corrections for host-galaxy reddening. Host-galaxy reddening corrections are not applied to the normal and 91bg-like type Ia SNe as they are not available. As a result there is likely some excess scatter in the curves traced by both the normal and 91bg-like Ia SNe samples in Figure 8.

The relatively tight locus for O2cx-like color evolution, shown in the left panel of Figure 8, reveals a previously unknown characteristic of the class. At peak, O2cx-like SNe are very blue similar to normal type Ia SNe (see the left box plot in Figure 8). While the blue color of O2cx-like SNe near maximum light has clearly been established (e.g., Foley et al. 2013), the tight scatter, ~ 0.2 mag, in $g' - r'$ at all epochs in the first ~ 20 d after peak suggests a common evolution.

Similar to the correlation between ejecta velocity and luminosity first noted by McClelland et al. (2010), SN 2009ku stands out as a clear outlier from the majority of the O2cx-like class. To bring SN 2009ku in line with the rest of the O2cx-like sample would require a host-galaxy reddening of $E(B - V) \approx 0.35$ mag, which would, in turn, make SN 2009ku ~ 1.2 mag brighter in the g' -band. In this scenario, SN 2009ku would be as luminous, or more luminous, than many normal type Ia SNe. As the sample of O2cx-like SNe grows, the similarity of SN 2009ku to the rest of the class should be closely monitored to determine if SN 2009ku belongs to a new subclass of low-velocity SNe Ia, separate from the other O2cx-like objects.

In addition to following a nearly uniform color curve, O2cx-like SNe exhibit unique $g' - r'$ evolution when compared to normal and 91bg-like type Ia SNe. The right panel of Figure 8 shows the change in $g' - r'$ color relative to $g' - r'$ at $T_{B,\text{max}}$. This normalization enables a measurement of the color evolution that is independent of line-of-sight extinction. It shows that O2cx-like and 91bg-like SNe become significantly redder in the first ~ 10 d after maximum, while normal type Ia SNe exhibit nearly constant $g' - r'$ color in the same timeframe. To measure this difference we define the change in $g' - r'$ color between maximum and +10 d, $\Delta(g' - r')_{10}$. The right inset in Figure 8 shows that 91bg-like and O2cx-like SNe have similar $\Delta(g' - r')_{10}$ values, while normal type Ia SNe have smaller $\Delta(g' - r')_{10}$ values. This, taken in combination with the $g' - r'$ color at peak, provides an empirical method for selecting O2cx-like SNe. At the time of maximum O2cx-like SNe are blue, like normal SNe Ia and unlike 91bg-like SNe, yet they exhibit large $\Delta(g' - r')_{10}$ values, similar to 91bg-like SNe and unlike normal SNe Ia.

The $g' - r'$ color evolution of O2cx-like SNe has important implications for future surveys, such as ZTF and

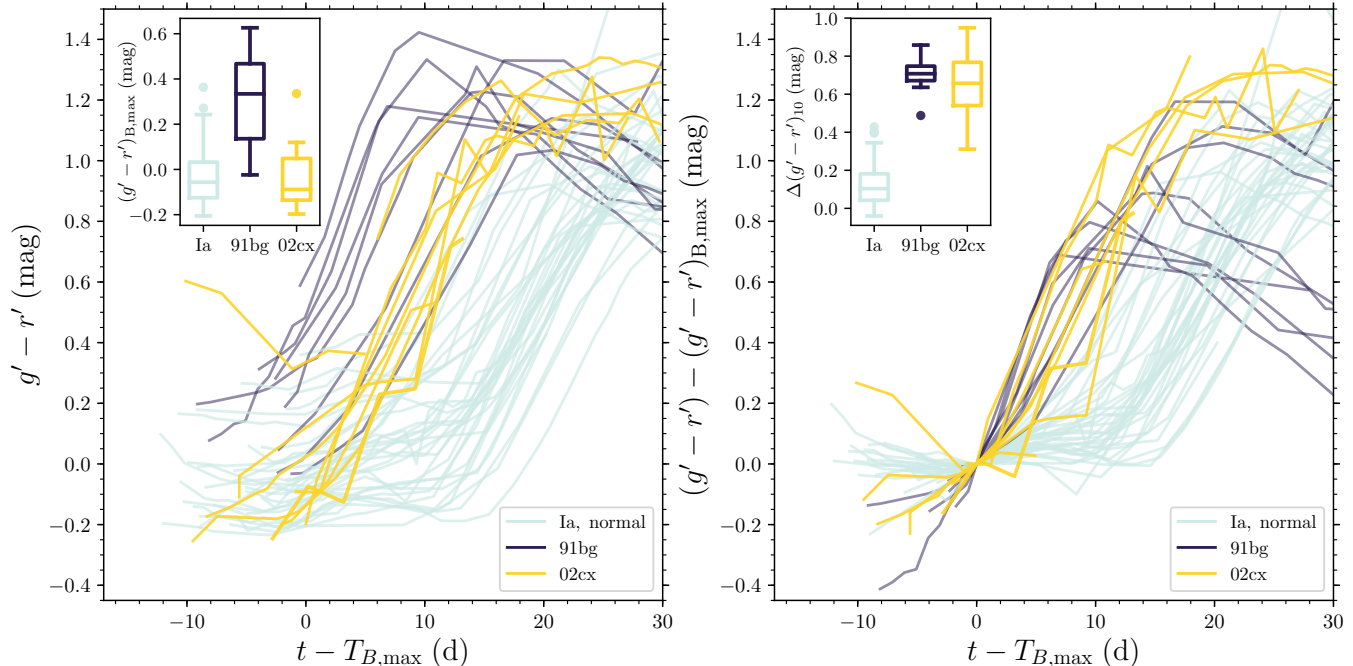


Figure 8. Color evolution of normal (shown in light blue), 91bg-like (purple) and 02cx-like (yellow) type Ia SNe. For clarity, photometric uncertainties are not shown and the individual measurements are connected via solid lines. The color curves are normalized to $T_{B,\max}$, where available (see text). The color curves are corrected for Galactic extinction, and in some cases host-galaxy extinction as well (see text). The samples for each subclass are defined in the text. The 02cx-like SNe 2009ku and 2010ae feature gaps in their $g' - r'$ color curves from $\sim +5$ d to $+30$ d and $\sim +11$ d to $+45$ d, respectively (Narayan et al. 2011; Stritzinger et al. 2014). As such, we only display these color curves through $+5$ d and $+11$ d, respectively.

Left: The $g' - r'$ color evolution of type Ia SNe. The 02cx-like SNe form a remarkably tight sequence with blue colors ($g' - r' \lesssim 0$ mag) at peak, and a rapid decline relative to normal type Ia SNe. SN 2009ku, which has $g' - r' \approx 0.6$ mag at -10 d, stands out as an outlier relative to the other 02cx-like SNe. The inset shows an inter-quartile range (IQR) box plot comparing the $g' - r'$ color at $T_{B,\max}$, determined via linear interpolation between the two epochs spanning $T_{B,\max}$, for the 3 subclasses. SN 2015H is excluded as the $g' - r'$ color is not available prior to $+6$ d (Magee et al. 2016). At peak, 02cx-like SNe are very blue (the red tail of the distribution is dominated by SN 2009ku) like normal Ia SNe, while 91bg-like SNe are red.

Right: The color evolution relative to the color at $T_{B,\max}$, denoted here as $(g' - r') - (g' - r')_{B,\max}$. By normalizing relative to the color at $T_{B,\max}$, we track the color evolution independent of line-of-sight extinction. The at B -maximum is determined via linear interpolation (see above). Both 91bg-like and 02cx-like SNe rapidly evolve to the red along a relatively tight sequence, independent of the temperature at peak. The inset IQR box plot shows the change in $(g' - r')$ color between $T_{B,\max}$ and $+10$ d, $\Delta(g' - r')_{10}$. The box plot clearly confirms that normal type Ia SNe remain blue longer than 91bg-like and 02cx-like SNe. SN 2009ku is excluded from the boxplot as there is no $(g' - r')$ measurement at $+10$ d (Narayan et al. 2011).

LSST. Spectroscopic completeness will be impossible for these surveys, but it will be possible to identify 02cx-like SNe from their $g' - r'$ color evolution alone. Using our sample of 9 02cx-like SNe, 9 91bg-like SNe, and 35 normal SNe Ia, we summarize the number of each that would be selected following hard cuts on $(g' - r')_{B,\max}$ and $\Delta(g' - r')_{10}$ in Table 3. While we generally advocate against hard cuts for target selection or classification (e.g., Miller et al. 2012), they illustrate the separation of the 02cx-like class in this case.

Table 3 shows that 02cx-like SNe are readily separated based on their $g' - r'$ evolution. For instance, adopting cuts of 0.0 and 0.5 (first column of Table 3) selects a pure sample of 02cx-like SNe, though less than half of the sample is recovered. Relaxing the cuts to 0.15 and 0.4 (third column) recovers more than half of the 02cx-like candidates, while still severely restricting the number of false positives.

Using the relative rate of 02cx-like SNe to normal type Ia SNe, 25% (see §5.3 below), and the relative rate of 91bg-like SNe to normal type Ia SNe, 19% (Li et al. 2011), we can estimate how many SNe would be selected by these cuts in a volume-limited sample. In a fixed volume with 100 normal SNe Ia we expect to find 19 91bg-

Table 3
Color Selection Results for 02cx-like SNe

SN type	$(g' - r')_{B,\max}$, $\Delta(g' - r')_{10}$			
	0.0, 0.5 ^a	0.1, 0.4 ^a	0.15, 0.4 ^a	0.15, 0.3 ^a
Normal Ia	0/35	2/35	2/35	4/35
91bg-like	0/9	2/9	3/9	3/9
02cx, obs. ^b	3/8	4/8	5/8	5/8
02cx, dered. ^c	4/8	6/8	6/8	7/8

Note. — Sources bluer than the $(g' - r')_{B,\max}$ cut and with a decline greater than the $\Delta(g' - r')_{10}$ cut are selected as candidate 02cx-like SNe. Our sample includes 9 02cx-like SNe, but SN 2015H is excluded due to a lack of $(g' - r')_{B,\max}$ measurement. SN 2009ku, which has $(g' - r')_{B,\max} \approx 0.34$ mag, is the only 02cx-like SNe that is not selected by any of the above cuts.

^a Respective cuts on $(g' - r')_{B,\max}$ and $\Delta(g' - r')_{10}$, in mag.

^b Recovered 02cx-like SNe when host-galaxy-reddening corrections are *not* applied.

^c Recovered 02cx-like SNe following host-galaxy reddening-corrections, as shown in Figure 8.

like SNe and 25 02cx-like SNe. If we apply cuts of 0.15 and 0.4 on $(g' - r')_{B,\max}$ and $\Delta(g' - r')_{10}$, respectively,

we would select $100 \times 2/35 \approx 6$ normal type Ia SNe, $19 \times 3/9 \approx 6$ 91bg-like SNe, and $25 \times 5/8 \approx 16$ 02cx-like SNe. This corresponds to a completeness of ~ 0.63 and a precision of ~ 0.56 . We caution that this example relies on uncertain rates (§5.3), and the assumption that our sample of SNe is representative of what would be found in a volume-limited survey. Starting next year ZTF will significantly reduce the uncertainties on both these assumptions. Nevertheless, this selection function for 02cx-like SNe will enable the efficient use of resources in the near future when transients are plentiful and follow-up scarce.

5.3. The Relative Rate of 02cx-like SNe

The controlled nature of the *Color Me Intrigued* experiment enables a unique estimate of the relative rate of 02cx-like SNe compared to type Ia SNe. Assuming 02cx-like SNe peak at $M \approx -15$ mag, then iPTF, which has a detection limit of $R_{\text{PTF}} \leq 20.5$ mag (Law et al. 2009), can detect these sources to a distance modulus $\mu = 35.5$ mag, corresponding to redshift $z \leq 0.03$. Below this redshift limit, there were 4 SNe Ia and 1 02cx-like SN, iPTF 16fnm, discovered during the course of the *Color Me Intrigued* experiment. Under the assumption of observational completeness, we therefore find that the relative rate of 02cx-like SNe to type Ia SNe, $r_{02\text{cx}/\text{Ia}}$, is $1/4 = 25\%$.

Prior to estimating the uncertainty on $r_{02\text{cx}/\text{Ia}}$, we caution that our assumption of observational completeness for 02cx-like SNe during the *Color Me Intrigued* experiment is likely overly optimistic. First, the luminosity function (LF) of 02cx-like SNe is poorly constrained. If the LF is heavily weighted towards extremely faint 08ha-like SNe, iPTF would have missed any of these beyond $z \approx 0.02$. Second, despite the high-cadence observations during *Color Me Intrigued*, the \sim week-long gaps in monitoring around full moon could have resulted in additional 02cx-like SNe that were missed. Third, our machine learning candidate identification software, *realbogus*, is limited by the flux contrast between the host galaxy and the SN. iPTF is complete to transients that are $> 10\times$ brighter than the underlying host surface brightness, but when the contrast drops to $0.7\times$ ($0.2\times$) the host galaxy surface brightness the completeness drops to $\sim 50\%$ ($\sim 2\%$), resulting in missed transients (Frohmaier et al. 2017, ApJ submitted). These concerns should not affect type Ia SNe, which are more luminous and long lived, meaning our $z \leq 0.03$ sample is potentially biased against 02cx-like SNe. Thus, the rate estimates included here are likely underestimates. Nevertheless, we proceed under the assumption that iPTF detected all $z \leq 0.03$ 02cx-like SNe during the *Color Me Intrigued* experiment.

Following the analysis presented in White et al. (2015), we can calculate confidence intervals for the relative rate of 02cx-like SNe to type Ia SNe. Given an outcome with probability p , the chances of getting k successes in a sample of n trials is given by the binomial distribution probability mass function:

$$Pr(k; n, p) = \binom{n}{k} p^k (1-p)^{n-k}. \quad (1)$$

Assuming a uniform prior $[0,1]$, the probability of p being less than some fiducial value p_0 given an observed

fraction k/n is

$$Pr(p < p_0; n, k) = \frac{\int_0^{p_0} Pr(k; n, p) dp}{\int_0^1 Pr(k; n, p) dp}. \quad (2)$$

From here, it follows that the probability that the relative rate $r_{02\text{cx}/\text{Ia}}$ is less than r_0 given $N_{02\text{cx}}$ 02cx-like SNe and N_{Ia} type Ia SNe is

$$Pr_{N_{02\text{cx}}, N_{\text{Ia}}}^{\text{rel}}(r_{02\text{cx}/\text{Ia}} < r_0) = Pr\left(p < \frac{r_0}{1+r_0}; N_{\text{SN}}, N_{02\text{cx}}\right), \quad (3)$$

where $N_{\text{SN}} = N_{\text{Ia}} + N_{02\text{cx}}$.

Considering SNe within the 02cx-like volume-limited sample (i.e., $z \leq 0.03$), we have $N_{\text{Ia}} = 4$ and $N_{02\text{cx}} = 1$. We find $Pr_{1,4}^{\text{rel}}(r < 100\%) = 95\%$ and $Pr_{1,4}^{\text{rel}}(r < 6.5\%) = 5\%$, which corresponds to a 90% confidence interval for the relative rate of $25_{-18.5}^{+75}\%$. In this case, small number statistics result in an estimate of the relative rate that is not particularly constraining. Nevertheless it is consistent with previous estimates including $\sim 5\%$ from Li et al. (2011), 5.6% from White et al. (2015), and 31% from Foley et al. (2013). While the methodologies differ, there is general agreement within the (large) uncertainties. Additionally, Li et al. note that their rate is likely underestimated if the luminosity function of 02cx-like SNe extends significantly fainter than SN 2005hk. Given that there are now many known 02cx-like SNe fainter than SN 2005hk (e.g., SNe 2008ha, 2007qd, 2010ae, iPTF 16fnm), it stands to reason that the true rate is likely higher than the estimate in Li et al. After limiting the survey volume to very nearby SNe, Foley et al. (2013) and White et al. (2015) apply correction factors of 2 and 1, respectively, to their relative rate measurements. The factor of 2 adopted in Foley et al. is highly uncertain, given the poorly-constrained LF of 02cx-like SNe and the many heterogeneous surveys used to define their sample of 02cx-like SNe. Meanwhile, the assumption that PTF was spectroscopically complete for slow-speed SNe, which is adopted in White et al., is likely overly optimistic. The true value of r^{rel} is likely between 0.05 and 0.3, and future surveys with large volumetric survey speeds (Bellm 2016), such as ZTF, are needed to significantly reduce the uncertainty on this measurement.

6. SUMMARY AND CONCLUSIONS

Maximizing information content while maintaining a large discovery rate is a challenge for modern wide-field time-domain surveys. This challenge will only be exacerbated in the coming years as extremely large field-of-view (ZTF) and large aperture (LSST) surveys come online. The looming orders-of-magnitude increase in discovered transients will overwhelm existing follow-up facilities and generate a “follow-up problem.” Ultimately this means survey telescopes will provide the sole observations of a majority of transients discovered in the coming decade. This near-future reality necessitates the immediate development of photometric-only methods for studying SNe and other transients.

To address the “follow-up problem” in the context of ZTF, we recently completed the *Color Me Intrigued* experiment during the final semester of iPTF. *Color Me Intrigued* searched for transients simultaneously in the

g_{PTF} and R_{PTF} filters, marking the first time this was done in PTF/iPTF. *Color Me Intrigued* addressed the “follow-up problem” in two critical ways: (i) the color information allowed us to identify extreme transients *at the epoch of discovery* by winnowing those with typical colors, ensuring only rare objects receive time-critical follow-up observations, and (ii) the strategy guaranteed that all newly discovered transients had color information at all epochs, which is critical for classifying sources without follow-up observations (e.g., [Poznanski et al. 2002](#)). As all PTF/iPTF surveys require two observations of the same field on a given night to reject asteroids as non-explosive transients, *Color Me Intrigued* provided a significant addition of information without a loss of survey area. As a precursor for LSST, we further employed a mixed cadence strategy whereby we cycled through 3 groups of fields each of which was observed with 1-d cadence for 1 lunation, and 3-d cadence at all other times. This mixed-cadence strategy was adopted to achieve a uniform depth across all fields at the end of the survey, while also monitoring variability on short and long timescales.

During the course of *Color Me Intrigued*, we discovered iPTF 16fnn, a new member of the 02cx-like subclass of type Ia SNe. iPTF 16fnn peaked at $M_{g_{\text{PTF}}} = -15.09 \pm 0.17$ mag and declined by ~ 1.2 mag in 13 d. The spectra of iPTF 16fnn were emblematic of the 02cx-like class, including the following properties: (i) very low velocity ejecta ($v_{\text{ej}} \approx 3000$ km s $^{-1}$), (ii) strong absorption from intermediate mass and Fe-group elements, and (iii) a not-fully nebular appearance several months after peak luminosity. Based on its photometric and spectroscopic evolution, iPTF 16fnn is an unambiguous member of the 02cx-like class.

We additionally compared iPTF 16fnn to other 02cx-like SNe, and find that it is among the least luminous members of the class. iPTF 16fnn is the second faintest known SN Ia, after SN 2008ha, which peaked at $M_g = -14.01 \pm 0.14$ mag ([Stritzinger et al. 2014](#)).²⁷ The post-peak spectra of iPTF 16fnn exhibit a striking resemblance to those of SNe 2007qd and 2010ae, with similar velocities and chemical compositions. These two SNe also peaked at $M \approx -15$ mag, and they exhibit a similar light curve evolution to iPTF 16fnn. The nearly identical evolution of these 3 SNe suggests a common origin.

Many studies have looked for correlated properties (luminosity, ejecta velocity, decline rate, etc.) to see if 02cx-like SNe can be described as a single-parameter family, similar to normal type Ia SNe. We update the previous work of [White et al. \(2015\)](#) and find that, at best, there is a weak correlation with large scatter between absolute magnitude and Δm_{15} in both the g' - and r' -bands. We also examine the $g' - r'$ color evolution of 02cx-like SNe, and compare it to normal and 91bg-like type Ia SNe. We find that 02cx-like SNe exhibit unique color evolution: blue colors at peak with large $\Delta(g' - r')_{10}$ values. While we do not have a physical explanation for this behavior, this empirical result can be used as a selection function for identifying 02cx-like SNe. We show that simple cuts

on $(g' - r')_{B,\text{max}}$ and $\Delta(g' - r')_{10}$ selects 02cx-like SNe with high completeness and precision. While limited by small number statistics, we nevertheless measure the relative rate of 02cx-like SNe to normal SNe Ia and find $r_{N_{02cx}/N_{\text{Ia}}} = 25^{+7.5}_{-18.5}\%$. This measurement is consistent with other estimates in the literature ([Li et al. 2011](#); [Foley et al. 2013](#); [White et al. 2015](#)).

In advance of ZTF, the *Color Me Intrigued* experiment has demonstrated that nightly observations in different filters can efficiently discover transients. In fact, the general success of this experiment has led to the decision to conduct the 3π ZTF public survey²⁸ with near-simultaneous g_{ZTF} and r_{ZTF} observations. The experiment has further shown the power of closely coupling efficient follow-up resources to survey telescopes. In particular, the SEDm correctly identified iPTF 16fnn as a low-velocity SN, despite its low spectral resolution ($R \approx 100$). Indeed, the SEDm model provides one potential path toward reducing the “follow-up problem” for LSST: building low-resolution spectrographs for 4-m class telescopes would enable efficient follow up for LSST transients with $r' \lesssim 22$ mag.

We close with a recommendation for future time-domain surveys. The search for astrophysical transients provides a fast moving target where new phenomena are regularly uncovered. These new discoveries often require new observational strategies to efficiently increase the sample size of these rarities. Due to its unique aperture and survey capabilities, early observations from LSST will likely uncover new phenomena.²⁹ If the LSST observational strategy is fixed without flexibility from the start of the survey, then the transient discoveries in year 2 will look like those from year 1, while year 3 will look like year 2, and so on. This scenario is detrimental for the exploration of explosive systems. By emphasizing a change in cadence at periodic intervals, iPTF was able to specifically target rare sources identified by PTF (e.g., the extensive use of 1-d cadence to find more young SNe similar to PTF 11kly/SN 2011fe; [Nugent et al. 2011](#); [Bloom et al. 2012a](#); [Cao et al. 2016b](#)), while also enabling new methods of exploration, such as *Color Me Intrigued*. Thus, we advocate the adoption of some measure of flexibility in the observational strategy of LSST. Even if minor, this flexibility may prove crucial to better understanding the nature of unusual sources discovered in the early stages of LSST.

Facilities: PO:1.2m, PO:1.5m (SEDm), Hale (DBSP), NOT (ALFOSC), Keck:I (LRIS)

©2017. All rights reserved.

We thank K. Shen for a useful discussion on the color evolution of Type Ia SNe. R. Amanullah pointed us to several useful papers on the color evolution of Type Ia SNe, for which we are grateful. Finally, we thank

²⁸ ZTF is a public-private partnership with 40% of the telescope time dedicated to a public survey. The public survey will monitor the full sky observable from Palomar Observatory with a 3-d cadence.

²⁹ To highlight an example from PTF, commissioning observations resulted in the discovery of 3 super-luminous SNe ([Quimby et al. 2011](#)). The [Quimby et al.](#) result established a new class of stellar explosion, while also explaining the nature of SCP 06F6 ([Barbary et al. 2009](#)), the most mysterious optical transient known at that time.

²⁷ Small changes in the reddening corrections or distance moduli to SN 2007qd or SN 2010ae could shuffle the order of the 2nd, 3rd, and 4th least luminous SNe Ia.

J. Nordin for examining the spectra of type Ia SNe found during *Color Me Intrigued*.

The Intermediate Palomar Transient Factory project is a scientific collaboration among the California Institute of Technology, Los Alamos National Laboratory, the University of Wisconsin, Milwaukee, the Oskar Klein Center, the Weizmann Institute of Science, the TANGO Program of the University System of Taiwan, and the Kavli Institute for the Physics and Mathematics of the Universe. This work was supported by the GROWTH project funded by the National Science Foundation under Grant No 1545949. Part of this research was carried out at the Jet Propulsion Laboratory, California Institute of Technology, under a contract with NASA.

Some of the data presented here were obtained in part with ALFOSC, which is provided by the Instituto de Astrofísica de Andalucía (IAA) under a joint agreement with the University of Copenhagen and NOTSA.

Some of the data presented herein were obtained at the W.M. Keck Observatory, which is operated as a scientific partnership among the California Institute of Technology, the University of California and NASA. The Observatory was made possible by the generous financial support of the W.M. Keck Foundation.

The authors wish to recognize and acknowledge the very significant cultural role and reverence that the summit of Mauna Kea has always had within the indigenous Hawaiian community. We are most fortunate to have the opportunity to conduct observations from this mountain.

This research has made use of the NASA/IPAC Extragalactic Database (NED), which is operated by the Jet Propulsion Laboratory, California Institute of Technology, under contract with NASA.

REFERENCES

- Astier, P., Guy, J., Regnault, N., et al. 2006, *A&A*, **447**, 31
- Barbary, K., Dawson, K. S., Tokita, K., et al. 2009, *ApJ*, **690**, 1358
- Bellm, E. C. 2016, *PASP*, **128**, 084501
- Bellm, E. C., Prince, T. A., Miller, A., et al. 2016, in American Astronomical Society Meeting Abstracts, Vol. 227, American Astronomical Society Meeting Abstracts, 421.07
- Ben-Ami, S., Konidaris, N., Quimby, R., et al. 2012, in *Proc. SPIE*, Vol. 8446, *Ground-based and Airborne Instrumentation for Astronomy IV*, 844686
- Blagorodnova, N., Gezari, S., Hung, T., et al. 2017, ArXiv e-prints, [arXiv:1703.00965](https://arxiv.org/abs/1703.00965) [[astro-ph.HE](https://arxiv.org/abs/1703.00965)]
- Blondin, S., & Tonry, J. L. 2007, *ApJ*, **666**, 1024
- Bloom, J. S., Kasen, D., Shen, K. J., et al. 2012a, *ApJ*, **744**, L17
- Bloom, J. S., Richards, J. W., Nugent, P. E., et al. 2012b, *PASP*, **124**, 1175
- Brink, H., Richards, J. W., Poznanski, D., et al. 2013, *MNRAS*, **435**, 1047
- Cao, Y., Kulkarni, S. R., Gal-Yam, A., et al. 2016a, *ApJ*, **832**, 86
- Cao, Y., Nugent, P. E., & Kasliwal, M. M. 2016b, *PASP*, **128**, 114502
- Cenko, S. B., Kulkarni, S. R., Horesh, A., et al. 2013, *ApJ*, **769**, 130
- Chambers, K. C., Magnier, E. A., Metcalfe, N., et al. 2016, ArXiv e-prints, [arXiv:1612.05560](https://arxiv.org/abs/1612.05560) [[astro-ph.IM](https://arxiv.org/abs/1612.05560)]
- Cook, D. O., Kasliwal, M. M., Van Sistine, A., et al. 2017, in American Astronomical Society Meeting Abstracts, Vol. 229, American Astronomical Society Meeting Abstracts, 237.08
- Filippenko, A. V. 1997, *ARA&A*, **35**, 309
- Fink, M., Kromer, M., Seitzzahl, I. R., et al. 2014, *MNRAS*, **438**, 1762
- Folatelli, G., Morrell, N., Phillips, M. M., et al. 2013, *ApJ*, **773**, 53
- Foley, R. J., Brown, P. J., Rest, A., et al. 2010, *ApJ*, **708**, L61
- Foley, R. J., Chornock, R., Filippenko, A. V., et al. 2009, *AJ*, **138**, 376
- Foley, R. J., Challis, P. J., Chornock, R., et al. 2013, *ApJ*, **767**, 57
- Frieman, J. A., Bassett, B., Becker, A., et al. 2008, *AJ*, **135**, 338
- Ganeshalingam, M., Li, W., Filippenko, A. V., et al. 2012, *ApJ*, **751**, 142
- Hillebrandt, W., Kromer, M., Röpke, F. K., & Ruiter, A. J. 2013, *Frontiers of Physics*, **8**, 116
- Ivezić, Ž., Tyson, J. A., Acosta, E., et al. 2008, ArXiv e-prints, [arXiv:0805.2366](https://arxiv.org/abs/0805.2366)
- Jones, D. O., Scolnic, D. M., Riess, A. G., et al. 2016, ArXiv e-prints, [arXiv:1611.07042](https://arxiv.org/abs/1611.07042)
- Kasliwal, M. M. 2011, PhD thesis, California Institute of Technology
- . 2012, *PASA*, **29**, 482
- Kessler, R., Marriner, J., Childress, M., et al. 2015, *AJ*, **150**, 172
- Kromer, M., Fink, M., Stanishev, V., et al. 2013, *MNRAS*, **429**, 2287
- Kulkarni, S. R. 2013, The Astronomer’s Telegram, 4807
- Kulkarni, S. R. 2016, in American Astronomical Society Meeting Abstracts, Vol. 227, American Astronomical Society Meeting Abstracts, 314.01
- Law, N. M., Kulkarni, S. R., Dekany, R. G., et al. 2009, *PASP*, **121**, 1395
- Li, W., Filippenko, A. V., Chornock, R., et al. 2003, *PASP*, **115**, 453
- Li, W., Leaman, J., Chornock, R., et al. 2011, *MNRAS*, **412**, 1441
- Lira, P. 1996, Master’s thesis, MS thesis. Univ. Chile (1996)
- Magee, M. R., Kotak, R., Sim, S. A., et al. 2016, *A&A*, **589**, A89
- . 2017, ArXiv e-prints, [arXiv:1701.05459](https://arxiv.org/abs/1701.05459) [[astro-ph.HE](https://arxiv.org/abs/1701.05459)]
- Masci, F. J., Laher, R. R., Rebbapragada, U. D., et al. 2017, *PASP*, **129**, 014002
- Mazzali, P. A., Röpke, F. K., Benetti, S., & Hillebrandt, W. 2007, *Science*, **315**, 825
- McClelland, C. M., Garnavich, P. M., Galbany, L., et al. 2010, *ApJ*, **720**, 704
- Miller, A. A., Richards, J. W., Bloom, J. S., et al. 2012, *ApJ*, **755**, 98
- Moriya, T., Tominaga, N., Tanaka, M., et al. 2010, *ApJ*, **719**, 1445
- Mould, J. R., Huchra, J. P., Freedman, W. L., et al. 2000, *ApJ*, **529**, 786
- Narayan, G., Foley, R. J., Berger, E., et al. 2011, *ApJ*, **731**, L11
- Nugent, P. E., Sullivan, M., Cenko, S. B., et al. 2011, *Nature*, **480**, 344
- Ofek, E. O., Laher, R., Law, N., et al. 2012, *PASP*, **124**, 62
- Oke, J. B., & Gunn, J. E. 1982, *PASP*, **94**, 586
- Oke, J. B., Cohen, J. G., Carr, M., et al. 1995, *PASP*, **107**, 375
- Perlmutter, S., Aldering, G., Goldhaber, G., et al. 1999, *ApJ*, **517**, 565
- Phillips, M. M. 1993, *ApJ*, **413**, L105
- Phillips, M. M., Lira, P., Suntzeff, N. B., et al. 1999, *AJ*, **118**, 1766
- Phillips, M. M., Li, W., Frieman, J. A., et al. 2007, *PASP*, **119**, 360
- Poznanski, D., Gal-Yam, A., Maoz, D., et al. 2002, *PASP*, **114**, 833
- Quimby, R. M., Kulkarni, S. R., Kasliwal, M. M., et al. 2011, *Nature*, **474**, 487
- Riess, A. G., Filippenko, A. V., Challis, P., et al. 1998, *AJ*, **116**, 1009
- Schlafly, E. F., & Finkbeiner, D. P. 2011, *ApJ*, **737**, 103
- Schlegel, D. J., Finkbeiner, D. P., & Davis, M. 1998, *ApJ*, **500**, 525
- Shappee, B. J., Prieto, J. L., Grupe, D., et al. 2014, *ApJ*, **788**, 48
- Stritzinger, M. D., Hsiao, E., Valenti, S., et al. 2014, *A&A*, **561**, A146
- Stritzinger, M. D., Valenti, S., Hoefflich, P., et al. 2015, *A&A*, **573**, A2
- Valenti, S., Pastorello, A., Cappellaro, E., et al. 2009, *Nature*, **459**, 674
- Wang, X., Filippenko, A. V., Ganeshalingam, M., et al. 2009, *ApJ*, **699**, L139
- Wegner, G., Haynes, M. P., & Giovanelli, R. 1993, *AJ*, **105**, 1251
- White, C. J., Kasliwal, M. M., Nugent, P. E., et al. 2015, *ApJ*, **799**, 52
- Yaron, O., & Gal-Yam, A. 2012, *PASP*, **124**, 668